# SAXS EXPERIMENTS ON GEL-SPUN POLYETHYLENE FIBERS

Hoogsteen, W.; Pennings, A.J.; Brinke, G. ten

*Published in:*
Colloid and Polymer Science

*DOI:*
10.1007/BF01490249

**Colloid & Polymer Science** Colloid Polym Sci 268:245–255 (1990)

# SAXS experiments on gel-spun polyethylene fibers

W. Hoogsteen, A. J. Pennings and G. ten Brinke

Department of Polymer Chemistry, University of Groningen, Groningen, The Netherlands

*Abstract:* The properties of gel-spun polyethylene fibers hot-drawn to the maximum draw ratio depend on the spinning conditions. Different spinning conditions result in two types of structure in the paraffin oil containing fibers: an isotropic lamellar structure or a shish-kebab structure. Meridional SAXS experiments can identify the structure present. After extraction, these structures are still present but can be detected only in a more indirect way by SAXS experiments because of an excessive contribution of void scattering. During hot-drawing both structures are transformed into a more fibrillar structure. The shish-kebab structures can be drawn only to relatively low hot-draw ratios with an incomplete transformation of the lamellar overgrowth into the fibrils, as demonstrated by the presence of a meridional SAXS maximum/shoulder. This leads to relatively weak fibers. Lamellar structures can be drawn to high draw ratios by chain unfolding. A nearly complete transformation of the lamellae into fibrils is obtained and the fibers have excellent properties. The information about the morphology obtained by SAXS, DSC, WAXS, and SEM can be used to establish a relation between morphology and properties.

*Key words:* Fibers; polyethylene; gel-spinning; small angle x-ray scattering; spinning conditions.

## 1. Introduction

There are a number of techniques available to prepare ultra-high strength polyethylene fibers [1–3]. Using routes that apply semi-dilute solutions as an intermediate stage [4–7] may potentially result in fibers with better properties than fibers prepared from more concentrated solutions [8–10]. Whether or not the favorable starting point of such a dilute entanglement system is utilized [11–13], depends on the optimalization of the processing conditions.

In our laboratory ultra-high strength polyethylene fibers are produced by the gel-spinning process using a 1–5 wt% solution of polyethylene in paraffin oil. Extrusion of this solution through a conical die at high temperatures yields a paraffin oil containing fiber. The paraffin oil is removed by extraction with n-hexane. After drying the fiber is hot-drawn to the maximum obtainable draw ratio which can be accompanied by a large improvement of its properties. However, in previous papers we showed that the ultimate properties depend strongly on spinning conditions such as spinning speed, spinning temperature, stretching in the spinline [14], molecular weight/weight distribution, polymer concentration [15], solvent quality and die geometry [16]. Moreover, in search for the explanation of these observations the morphology of these fibers has been studied by wide-angle x-ray scattering (WAXS), scanning electron microscopy (SEM), differential scanning calorimetry (DSC) [17], and some small-angle x-ray scattering (SAXS) experiments [18].

The main conclusions can be summarized as follows. High deformation rates in the spinline lead to shish-kebab structures, first at the periphery of the spinline, which after hot-drawing lead to fibers with low tensile strengths. Therefore, spinline stretching should be avoided especially at relatively low spinning temperatures [14]. The presence of a low temperature melting endotherm in the DSC thermograms of melting experiments on constrained weak fibers shows that these fibers still contain a considerable amount of lamellar material which most probably bears no load during stress strain experiments [17]. Besides the amount of lamellar material, the length of the crystal blocks also plays an important role with respect to the strength of the fiber. Longer crystal blocks prevent creep failure up to higher stresses since the orthorhombic to hexagonal solid solid phase transition, after which chain slippage can occur, is involved in the fracture mechanism [19]. A one-to-one correspondence between a higher orthorhombic to hexagonal solid solid phase transition temperature and a higher tensile strength is observed [17].

In this paper the results of a systematic small angle x-ray scattering study of gelspun polyethylene fibers prepared at different spinning conditions will be presented. Different stages of the preparation process (paraffin oil containing fiber, extracted fiber an hot-drawn fiber) will be considered separately. In this way the conclusions about the relation between morphology and properties drawn before will be confirmed and complementary information will be obtained.

## 2. Experimental

Two samples of linear polyethylene Hifax 1900 were used, one with a broad molecular weight distribution ($\overline{M}_w$ = $4 \times 10^6$ kg/kmol, $\overline{M}_w/\overline{M}_n \approx 20$; referred to as HifaxA) and one with a narrow molecular weight distribution ($\overline{M}_w = 5.5 \times 10^6$ kg/kmol, $\overline{M}_w/\overline{M}_n \approx 3$; referred to as HifaxB). 1–5 wt% polyethylene solutions in paraffin oil were prepared (containing 0.5 wt% 2,6-di-t-butyl, 4-methylcresol anti-oxidant) at 150 °C. Upon cooling this solution forms a gel which was fed to the spinning apparatus. The gel was extruded into a filament at temperatures varying from 170 ° to 250 °C with an extrusion rate of 1 or 100 m/min, using a conical die with an exit of 1 mm [16]. The paraffin oil was extracted from these filaments with n-hexane. Afterwards, hot-drawing to different draw ratios was carried out at a temperature in the range of 144 °C–148 °C in a nitrogen atmosphere.

For the scattering experiments (WAXS/SAXS) CuK$\alpha$ radiation $\lambda$ = 0.154 nm) was used, produced by a Philips x-ray generator connected to a closed cooling circuit and operated at 45 kV and 45 mA. SAXS experiments were carried out using a Kratky camera equipped with a proportional counter and an electronic stepscanner. Monochromatization was achieved by using a Ni filter and pulse height discrimination. Usually, the entrance slit was 80 $\mu$m (in some cases also 40 $\mu$m; this will be indicated in the text). In the case of equatorial measurements one single fiber was aligned accurately with the fiber axis parallel to the slit, whereas for meridional measurements fibers were placed next to each other over the length of the x-ray beam perpendicular to the plane of the beam by winding a fiber on a rectangular frame. In the last case many cross-sections are irradiated. It should be noticed that in this way two layers of fibers are obtained, slightly displaced by the frame thickness, and that the fiber turns are inclined a little with respect to the vertical as a result of the pitch. WAXS measurements were carried out using a Statton camera (pinhole collimation). This camera was also used for some SAXS measurements (sample to film distance 31 cm).

## 3. Results and discussion

### 3.1. *SAXS of the paraffin oil containing gel-spun polyethylene fibers*

The paraffin oil containing fiber ist the first intermediate product in the production process of strong polyethylene fibers. It is obtained after extrusion and quenching a semi-dilute solution of polyethylene. In Fig. 1 the equatorial SAXS curves are presented for three fibers prepared at different spinning conditions.

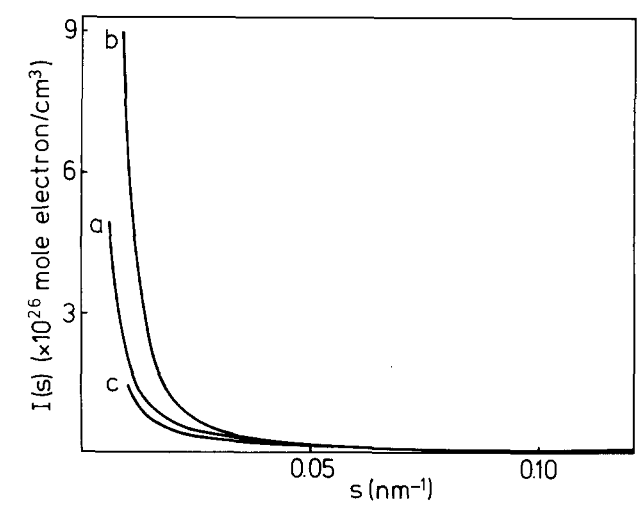


Fig. 1. Equatorial SAXS intensity curves of paraffin oil containing gel-spun polyethylene fibers prepared at different spinning conditions. For curve a and b a 40 $\mu$m entrance slit was used. a) $T_{spin}$ = 170 °C, $V_{spin} = V_{wind}$ = 100 m/min, 5 wt% HifaxA; b) $T_{spin}$ = 170 °C, $V_{spin}$ = 100 m/min, $V_{wind}$ = 1000 m/min, 5 wt% HifaxA; c) $T_{spin}$ = 190 °C, $V_{spin} = V_{wind}$ = 1 m/min, 1.5 wt% HifaxB.

The equatorial slit smeared intensity is scaled to an absolute intensity scale using a Lupolen polyethylene sample (in this paper only slit-smeared intensities are dealt with because desmearing is only possible for isotropic samples). This can create problems when the dimension of the fiber cross-section is of the same order as the width of the primary beam at the sample position. The width of the primary beam depends on the width of the entrance slit. The dimension of the paraffin oil containing fiber is determined by the diameter of the die and the degree of stretching in the spinline. Fortunately, in the case of paraffin oil containing fibers the dimensions exceed the width of the primary beam at the sample position since a die with a diameter of 1 mm is used and the spinline draw ratio is at most 10. The diameter of the fibers is estimated from a combination of a rough diameter determination using a microscope and the calculation from the measured transmission. In the latter case a linear absorbtion coefficient of 4.0 $cm^{-1}$ for polyethylene as well as paraffin oil and uniform thickness is assumed. In this way a reasonable approximation of the absolute intensity is obtained.

The equatorial intensity decreases continuously with increasing scattering angle for all fibers. However, the intensity of the fibers stretched in the spinline (Fig. 1b) is considerably higher than for the unstretched fibers (Fig. 1a, 1c). This can be accounted for in the following way. The paraffin oil containing fiber may be considered as a three-phase system consisting of amorphous polyethylene, crystalline polyethylene, and paraffin oil with densities of, resp., 0.855, 1.000, and 0.845 $g/cm^3$. This corresponds to, resp., 0.489, 0.571, and 0.483 mole electron/$cm^3$. The scattering power $\overline{\eta^2}$ is given by

$$\overline{\eta^2} = \omega_c \omega_a (\rho_c - \rho_a)^2 + \omega_c \omega_p (\rho_c - \rho_p)^2 + \omega_a \omega_p (\rho_a - \rho_p)^2, \tag{1}$$

where $\omega_c$, $\omega_a$, and $\omega_p$ are the volume fractions of crystalline polyethylene, amorphous polyethylene, and paraffin oil. $\rho_c$, $\rho_a$, and $\rho_p$ are the electron densities (mole electron/$cm^3$) for these components. The value of $\omega_p$ ist very high and $\omega_c$ and $\omega_a$ are both small. During the extrusion process some oil is squeezed out. The amount involved increases for spinline stretching, leading to a lower value of $\omega_p$ and higher values of $\omega_a$ and $\omega_c$. As a consequence a higher equatorial intensity is found.

Fig. 2 shows the meridional intensity curves of paraffin oil containing fibers prepared at various spinning conditions. Since no absolute intensities can be obtained for meridional measurements, the intensity curves for different paraffin oil containing fibers

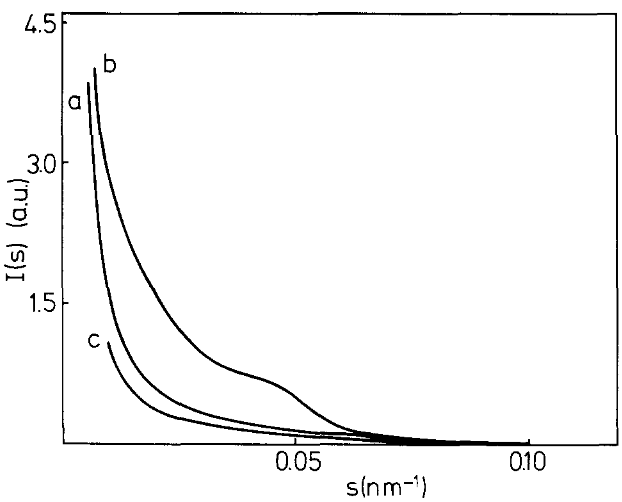


Fig. 2. Meridional SAXS intensity curves of paraffin oil containing gel-spun polyethylene fibers prepared at different spinning conditions. For curve a and b a 40 $\mu m$ entrance slit was used. a) $T_{spin}$ = 170 °C, $V_{spin} = V_{wind}$ = 100 m/min, 5 wt% HifaxA; b) $T_{spin}$ = 170 °C, $V_{spin}$ = 100 m/min, $V_{wind}$ = 1000 m/min, 5 wt% HifaxA; c) $T_{spin}$ = 190 °C, $V_{spin} = V_{wind}$ = 1 m/min, 1,5 wt% HifaxB.

are scaled with respect to each other using an apparent thickness calculated from the measured transmission. The scattering curve of the fiber stretched in the spinline at a relatively low spinning temperature (Fig. 2b) contains a shoulder. The corresponding Bragg value is about 22 nm. It has been shown [14, 15, 18] that these kind of fibers show a preferential c-axis orientation parallel to the fiber axis ascribed to the formation of shish-kebab structures as a result of the high deformation rates involved. Furthermore, these kinds of intermediate structures lead to fibers with poor properties after extraction and hot-drawing. The shoulder in the meridional scattering curve can be ascribed to particle scattering of the crystalline parts of the lamellae in the overgrowth of the shish-kebabs. This scattering contribution shows up because the crystalline blocks are surrounded by a matrix of lower electron density consisting of amorphous polyethylene and voids filled with paraffin oil. Apparently, it behaves as a more or less dilute system.

For fibers containing no preferential c-axis orientation (unstretched or spinline stretched at high spinning temperatures) no meridional shoulder is observed. From these intermediates, fibers with good properties can be obtained.

### 3.2. SAXS of the extracted gel-spun polyethylene fibers

The extracted fiber is the second intermediate of the gel-spinning process in a route to high strength polyethylene fibers. The effect of the extraction process on the morphology of the fibers has been discussed before [18]. Usually hexane is used to remove the paraffin oil. During the fast evaporation of hexane longitudinal shrinkage ist prevented and local high stress concentrations occur, leading to a craze-type of void/fibril formation. If, instead, a less volatile solvent like decalin is used, a reduction of the local stress concentrations occurs and void formation is avoided. Moreover, due to the fixed length constraint, the lamellae tilt and a preferential c-axis orientation perpendicular to the fiber axis is obtained. A close packing of lamellae oriented in this way leads to an equatorial SAXS maximum as long as the scattering is not dominated by the void scattering. If this occurs, the equatorial maximum can be brought out by filling the pores with paraffin oil. This structure of tilted lamellae with the c-axis perpendicular to the fiber axis is typical for fibers not spinline stretched or spinline stretched at high-spinning temperatures. They can be easily hot-drawn by the mechanism of chain unfolding. Extraction of fibers stretched in the spinline and containing shish-kebab structures always leads to porous fibers, even if decalin is used. Apparently, the shish-kebab structure is very stiff and lateral shrinkage during evaporation of the solvent is partly hampered.

Information about the porosity can be obtained if the equatorial intensities are scaled to an absolute intensity scale. This is more difficult for the extracted fibers than for the paraffin oil containing fibers since extraction leads to lateral shrinkage of the fibers. Especially in the case of spinline-stretched fibers the dimension of the fiber cross-section becomes smaller than the width of the primary beam. The primary beam profile in the direction perpendicular to the slit at the sample position is a triangular distribution in the case of complete illumination of the entrance slit, as can be calculated from the dimensions of the Kratky collimation. This was checked by measuring the primary beam profile at the detector position using a 20 $\mu m$ counter slit. The measured and calculated beam at the detector position agreed well. From the calculated triangular beam profile at the sample position absolute intensities were estimated. First the diameter was measured using a microscope and a micrometer. For the equatorial scattering experiments the fibers were aligned accurately with the fiber axis parallel to the slit in such a way that the highest intensity was obtained. The limited width of the fiber was taken into account by using only the relevant part of the primary beam profile at the sample position.

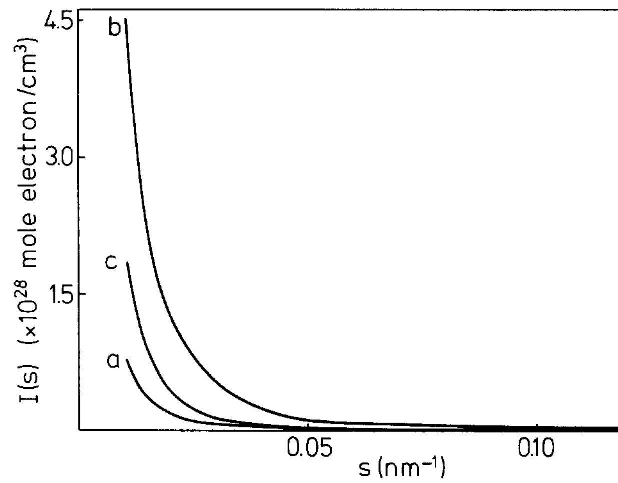


Fig. 3. Equatorial SAXS intensity curves of extracted gel-spun polyethylene fibers prepared at different spinning conditions from a 1,5 wt% HifaxB solution. a) $T_{spin}$ = 172 °C, $V_{spin}$ = $V_{wind}$ = 100 m/min; b) $T_{spin}$ = 172 °C, $V_{spin}$ = 100 m/min, $V_{wind}$ = 500 m/min; c) $T_{spin}$ = 200 °C, $V_{spin}$ = $V_{wind}$ = 1 m/min.

In Fig. 3 equatorial intensity curves on an absolute scale are presented for fibers prepared at different spinning conditions. The intensity decreases continuously with increasing scattering angle. The highest intensity is observed for the shish-kebab containing fiber (curve b) indicating that this spinline stretched fiber has a very porous structure. Fig. 3a shows the equatorial scattering curve of a fiber prepared from a 1.5 wt% polyethylene solution with a spinning speed and winding speed of 100 m/min. It has been observed before [15] that fibers prepared at these spinning conditions have a ribbon-like shape. The lamellae are preferentialy oriented with their large flat surface parallel to the large surface of the ribbons – a type of orientation which is also observed for mats of single crystals [20] and thin gel films [21–23]. This type of packing leads to relatively few voids and a low scattering intensity. The equatorial scattering curve in Fig. 3a is the result of a flat on measurement showing no equatorial maximum. In an equatorial measurement taken edge on, an equatorial

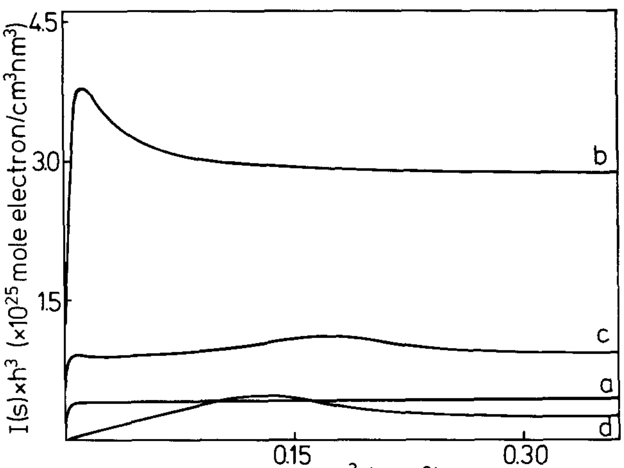


Fig. 4. Equatorial SAXS Porod curves of extracted gel-spun polyethylene fibers prepared at different spinning conditions. a) $T_{spin}$ = 172 °C, $V_{spin} = V_{wind}$ = 100 m/min, 1.5 wt% HifaxB; b) $T_{spin}$ = 172 °C, $V_{spin}$ = 100 m/min, $V_{wind}$ = 500 m/min, 1.5 wt% HifaxB; c) $T_{spin}$ = 200 °C, $V_{spin} = V_{wind}$ = 1 m/min, 1.5 wt% HifaxB; d) $T_{spin}$ = 230 °C, $V_{spin} = V_{wind}$ = 100 m/min, 5.0 wt% HifaxA.

maximum/shoulder due to a regular packing of the lamellae can be observed.

Fig. 4 shows the equatorial intensities of Fig. 3 multiplied by $h^3$ ($h = 2\pi s$, $s = 2\sin\theta/\lambda$) as a function of $h^3$. These Porod plots are very different for fibers prepared at different spinning conditions. This in contrast to the corresponding intensity curves presented in Fig. 3. Recently, Ciccariello etal. [24] showed that for two- and three-phase systems the angular region where Porod behavior can be observed depends on the characteristic lengths of the phases. Therefore, Porod curves can be useful to get information about the structure of these systems. Curve 4a is the Porod plot of the equatorial flat on measurement of a ribbon-like fiber with the lamellae preferentially oriented with their large flat surface parallel to the large ribbon surface. Since the direction of the incident x-ray beam is parallel to the normal of the lamellae, no contribution to the scattering due to the package of lamellae is expected. The scattering can approximately be ascribed to a two-phase system polyethylene/voids. The plateau in the Porod curve indicates that the interphase boundary can be considered as being sharp, i.e., a discrete valued electron density change; curve 4c also shows a plateau. However, there is a hump at a value $h^3$ = 0.18 nm$^{-3}$, which corresponds to a $s^{-1}$ value of 11 nm. It is approximately the same as the Bragg value of the equatorial SAXS maximum found for the intensity curves of fibers with a lamellar structure containing few voids or with the voids filled with paraffin oil. Apparently, the presence of lamellae oriented perpendicular to the fiber axis can be detected in a three-phase system with a high scattering contribution of the voids without the need to fill the pores with paraffin oil. Curve 4d shows the Porod plot of a nonporous extracted fiber. The corresponding intensity curve (not shown) has a clear equatorial maximum at about 12 nm. The Porod plot contains a clear maximum at $h^3$ = 0.14 mm$^{-3}$, which corresponds to a $s^{-1}$ value of 12 nm; however, no plateau is observed.

Curve 4b represents a characteristic Porod plot for fibers stretched in the spinline and containing a shish-kebab structure. A clear maximum is observed at $h^3$ = 0.015nm$^{-3}$ corresponding to a $s^{-1}$ value of 25 nm. It becomes more pronounced for increasing degree of c-axis orientation parallel to the fiber axis, but always at approximately the same position. Similar curves are obtained for particle scattering of particles with smooth surface in dilute solutions [25, 26] as well as concentrated systems [26]. The way in which the limiting Porod constant at large angles is approached depends strongly on the shape of the particles. For smooth particles the $I(h)h^3$ *vs* $h^3$ (or $h$) curves (also referred to as Porod's plot) exhibits a maximum. For particles with sharp edges the curve gradually approaches an asymptotic value. Therefore, the maximum in curve 4b most probably indicates that the structures responsible for the scattering have a smooth shape in the direction perpendicular to the fiber axis. For example, in the case of long fibrils oriented parallel to the fiber axis, the equatorial measurements give information about the (shape of the) lateral dimensions of the fibrils.

Attempts to get more structural information from the equatorial scattering curves, (as for instance the fibril diameter of the backbones of the shish-kebab containing fibers using the Guinier approximation, a method applied succesfully by van Hutten et al. for surface grown shish-kebab fibers [27]) failed because no straight line was obtained. Interference, a distribution of sizes, or the presence of different structures, each giving their own scattering contribution, could be responsible.

The meridional scattering curves of extracted fibers prepared at different spinning conditions are presented in Fig. 5. Very high intensities are found,

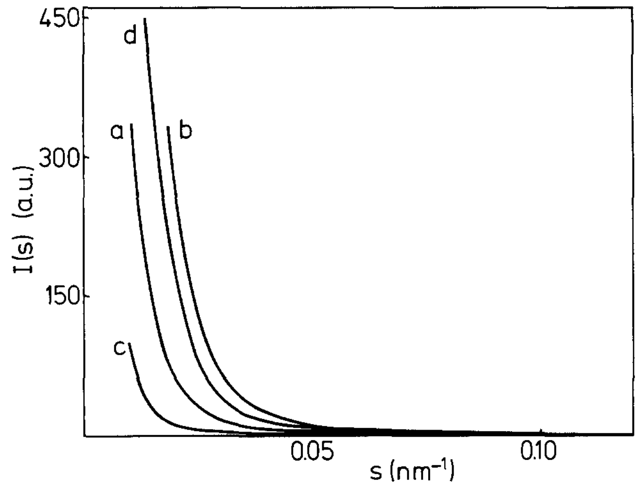


Fig. 5. Meridional SAXS intensity curves of extracted gel-spun polyethylene fibers prepared at different spinning conditions. a) $T_{spin}$ = 172 °C, $V_{spin}$ = $V_{wind}$ = 100 m/min, 1.5 wt% HifaxB; b )$T_{spin}$ = 180 °C, $V_{spin}$ = 100 m/min, $V_{wind}$ = 500 m/min, 1.5 wt% HifaxB; c) $T_{spin}$ = 170 °C, $V_{spin}$ = $V_{wind}$ = 1 m/min, 1.5 wt% HifaxB; d) $T_{spin}$ = 190 °C, $V_{spin}$ = 100 m/min, $V_{wind}$ = 500 m/min, 2.0 wt% HifaxA.

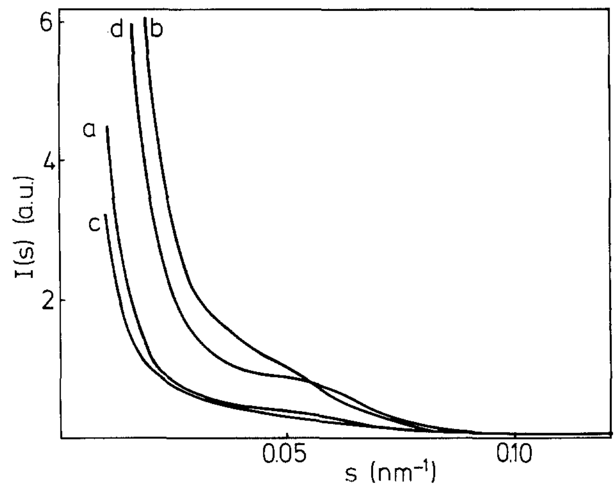


Fig. 6. Meridional SAXS intensity curves of extracted gel-spun polyethylene fibers prepared at different spinning conditions and afterwards filled with paraffin oil. a) $T_{spin}$ = 172 °C, $V_{spin}$ = $V_{wind}$ = 100 m/min, 1.5 wt% HifaxB; b) $T_{spin}$ = 180 °C, $V_{spin}$ = 100 m/min, $V_{wind}$ = 500 m/min, 1.5 wt% HifaxB; c) $T_{spin}$ = 170 °C, $V_{spin}$ = $V_{wind}$ = 1 m/min, 1.5 wt% HifaxB; d) $T_{spin}$ = 190 °C, $V_{spin}$ = 100 m/min, $V_{wind}$ = 500 m/min, 2.0 wt% HifaxA.

especially for the shish-kebab containing fibers (Fig. 5b and d). The intensities were scaled with respect to each other using the sample mass. The shoulder in the meridional intensity curve of paraffin oil containing fibers with shish-kebab structure (Fig. 2b), disappeared completely due to the intense void scattering. The intensity decreases continuously with increasing scattering angle for all fibers, also when a 40 $\mu$m slit, allowing measurements at smaller angles, was used. This is in contrast with shish-kebab fibers prepared by the surface-growth method which often showed a meridional maximum at an angular position corresponding to about 100 nm, and is due to a regular "packing" of voids and lamellae along the backbone of the shish-kebabs [27]. The absence of a corresponding maximum for gel-spun shish-kebab structures can be ascribed to the fiber preparation technique. In the case of surface-growth the crystallization takes place slowly and isothermally whereas gel-spinning is a relatively fast process where the fiber is cooled down from temperatures above 170 °C to room temperature very rapidly. This will result in more irregular structures along the backbone.

Filling the pores with paraffin oil again leads to a tremendous drop of the meridional intensities. This is demonstrated by Fig. 5 and 6, realizing that the relative intensities may be compared because the intensities are normalized with respect to the polyethylene sample mass. For the fibers stretched in the spinline and containing a shish-kebab structure the meridional shoulder reappears (Fig. 6b and d). It is more pronounced for the fiber prepared from the polyethylene sample with a relatively broad molecular weight distribution (HifaxA) than for the polyethylene sample with the narrower molecular weight distribution (HifaxB). The entanglement system of the last is more permanent on the time scale of the experiment, i.e., longer relaxation times. During the spinning process mainly the long chains remain stretched, whereas the short chains have returned to their isotropic state [28]. If more low molecular weight material is available, more material will be in the lamellar overgrowth and, as a consequence, a more pronounced shoulder will appear.

Curve 6a also contains a very faint shoulder indicating that some shish-kebab structure is present. This intensity curve belongs to a ribbon-like fiber spun at a relatively low spinning temperature with a spinning speed of 100 m/min without spinline stretching. It was observed previously that this fibers contain a thin shish-kebab-like skin [15], a surface structure most probably responsible for the faint

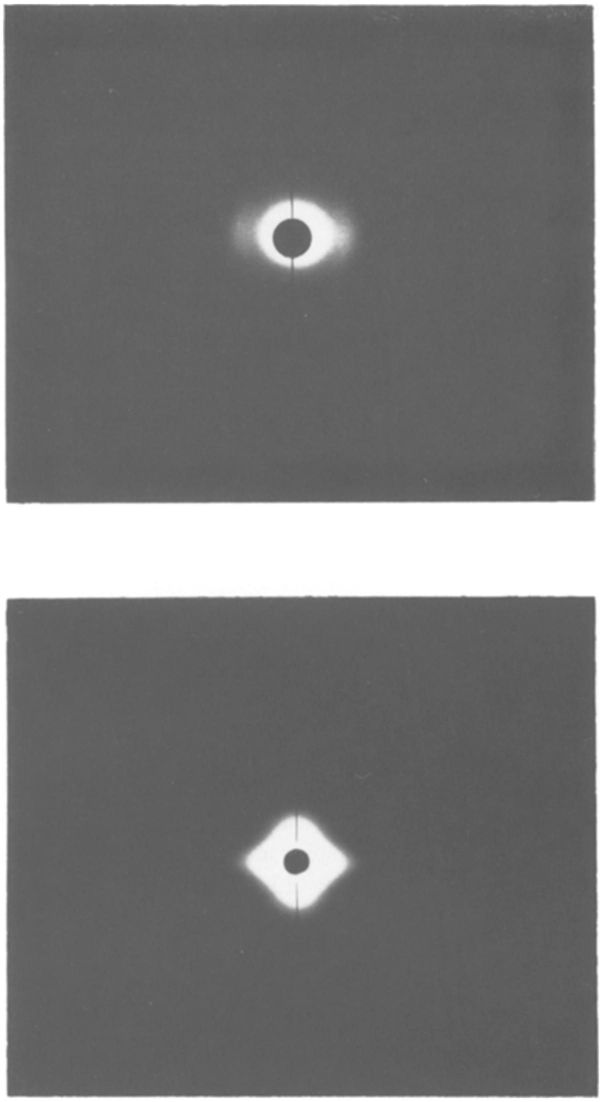

Fig. 7. SAXS pinhole patterns of extracted gel-spun polyethylene fibers prepared at different spinning conditions. Fiber axis vertical. a) $T_{spin}$ = 215 °C, $V_{spin}$ = $V_{wind}$ = 1 m/min, 5.0 wt% HifaxA; b) $T_{spin}$ = 180 °C, $V_{spin}$ = 100 m/min, $V_{wind}$ = 500 m/min, 1.5 wt% HifaxB.

shoulder observed. The presence of this structure results from small orientation effects due to the high extrusion rate and relatively low spinning speed. Orientation effects due to the extrusion rate become more pronounced at higher extrusion rates (up to 800 m/min) [29].

A disadvantage of the use of the Kratky camera for the study of oriented systems is the loss of information in the direction parallel to the slit. Therefore, measurements at many different sample orientations with respect to the slit are necessary to obtain all possible information. The restriction to equatorial and meridional experiments only may be insufficient in some cases. For this reason a pinhole camera was also used, in spite of some disadvantages like low intensities and larger minimum angles. Two examples are presented in Fig. 7. Fig. 7a is the pinhole pattern of a fiber not stretched in the spinline and containing few voids. A clear intensity maximum on an arc centered around the equator is observed. This picture confirms the conclusion drawn from the equatorial SAXS maximum observed with the Kratky camera [18]. In Fig. 7b the SAXS pinhole pattern of a shish-kebab containing spinline stretched fiber is presented. The diamond shape indicates that the morphology is strongly oriented. The high intensity results from the porous structure which is a consequence of the presence of lamellar overgrowth preventing a close packing of the backbone fibrils. A similar pinhole pattern was obtained for surface-growth fibers indicating that these structures are strongly related [27]. For fibers not stretched in the spinline more circular pinhole patterns are observed.

### 3.3. *SAXS of the hot-drawn gel-spun polyethylene fibers*

Hot-drawing is the final step in the gel-spinning process. During this step a large improvement of the fiber properties can be obtained. The maximum hot-draw ratio depends strongly on the morphology of the extracted fibers.

Spinline stretched fibers containing shish-kebab structure can only be drawn to small maximum hot-draw ratios. Values vary between 2 and 10, depending, among others, on the molecular weight distribution [17]. The plastic deformation of shish-kebabs has been extensively investigated with aid of SEM [30–32] and SAXS [33, 34]. It was observed that the lamellar overgrowth was gradually pulled into the backbone fibrils. The diameter of the fibrils (≈ 15 nm) was nearly independent of the draw ratio. Because the lateral dimension of the lamellar overgrowth was in the range of 100 nm, a complete transformation of the lamellar overgrowth into the fibrils was expected to occur for a hot-draw ratio of about 10 [31]. In practice such high draw ratios were often not obtained due to premature breakage, especially for surface-growth fibers [30].

The maximum hot-draw ratio for extracted fibers not stretched in the spinline is in the order of 100. The hot-drawing mechanism for this type of fibers has been investigated with SEM [31, 35] and SAXS [35]. SEM revealed that a relatively low drawing temperatures (120 °C) fibrils were formed in a way which looked very much like crazing in glassy polymers [36], whereas for higher drawing temperatures (144 °C) dense bundles of fibrils were pulled out from globular entities. At 120 °C a very porous structure was obtained, but after hot-drawing at 144 °C a dense structure with only some voids in the micron range due to lamellar melting recrystallization was found. The large lamellar regions from which the fibrils arise are less well defined than those for the case of overgrowth of shish-kebabs. Since the lateral dimensions of the lamellae are large and because they are preferentialy oriented with the c-axis perpendicular to the fiber axis, these fibers can be hot-drawn quite well to high draw ratios by chain unfolding. If these fibers are drawn to medium draw ratios shish-kebab-like structures are obtained due to recrystallization of unoriented parts along fibrils consisting of extended chain blocks. SAXS measurements of this type of structure reveal a meridional maximum and SEM photographs show a striated surface structure corresponding to a 40 nm period [35]. Such a fibril in matrix model is also found in melt-drawn polyethylene [37].

For fibers stretched in the spinline at relatively high spinning temperatures hot-draw ratios between 10 and 100 are obtained. The morphology of the extracted fibers prepared in this way is very similar to that of extracted fibers not stretched in the spinline [14, 15, 18]. It is not completely clear why the maximum hot-draw ratio is smaller. DSC experiments show [17] that the crystallinity of the extracted fibers is somewhat lower than for fibers not stretched in the spinline. Furthermore, the orthorhombic to hexagonal solid solid phase transition temperature in fibers drawn to the maximum hot-draw ratio, which is a measure for the length of the crystal blocks in the fibril, is also somewhat lower. Although a nearly complete transformation of the lamellar material into a fibrillar structure is obtained, the distance between regions with an accumulation of entanglements and the number of such regions apparently varies with the spinning conditions.

Fig. 8 shows the equatorial scattering curves of fibers prepared at different spinning conditions and drawn to different hot-draw ratios. The intensities are scaled to an absolute intensity scale in the same way as described for the extracted fibers. Because the hot-drawn fibers are very thin no reliable values for the thickness could be obtained with the micrometer. Therfore, thicknesses were calculated from the mass of the fibers using the width of the fiber as determined with a microscope and assuming uniform thickness. Another complication due to the small lateral dimensions of these fibers is a contribution to the scattering curve of reflection of the primary beam on the surface of the fiber [38, 39]. This effect turned out to be considerable for fibers with lateral dimensions smaller than about 30 $\mu$m, as will be shown and discussed more extensively in a subsequent paper [40]. In this paper only fibers with lateral dimensions larger than 30 $\mu$m are dealt with that in the case of high hot-draw ratios, were obtained by using a relatively high polymer concentration (e.g., curve 8d). The values of the absolute intensities are small (compare Fig. 3) indicating that upon hot-drawing the porous structure disappears, at least at a 100 nm scale, in agreement with results obtained earlier [35]. A more extensive discussion of the porosity will appear in a subsequent paper [40]. The equatorial scattering is very similar for fibers prepared at different spinning conditions and different hot-draw ratios.

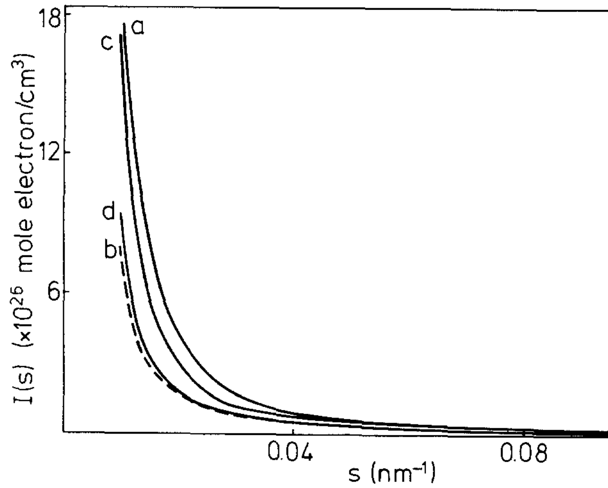


Fig. 8. Equatorial SAXS intensity curves of hot-drawn gel-spun polyethylene fibers prepared at different spinning conditions and drawn to different hot-draw ratios $\lambda$. a) $T_{spin}$ = 172 °C, $V_{spin} = V_{wind}$ = 100 m/min, 1.5 wt% HifaxB, $\lambda$ = 4; b) $T_{spin}$ = 180 °C, $V_{spin}$ = 100 m/min, $V_{wind}$ = 500 m/min, 1.5 wt% HifaxB, $\lambda$ = 2; c) $T_{spin}$ = 191 °C, $V_{spin} = V_{wind}$ = 1 m/min, 1.5 wt% HifaxB, $\lambda$ = 5; d) $T_{spin}$ = 170 °C, $V_{spin} = V_{wind}$ = 1 m/min, 5.0 wt% HifaxA, $\lambda$ = 100.

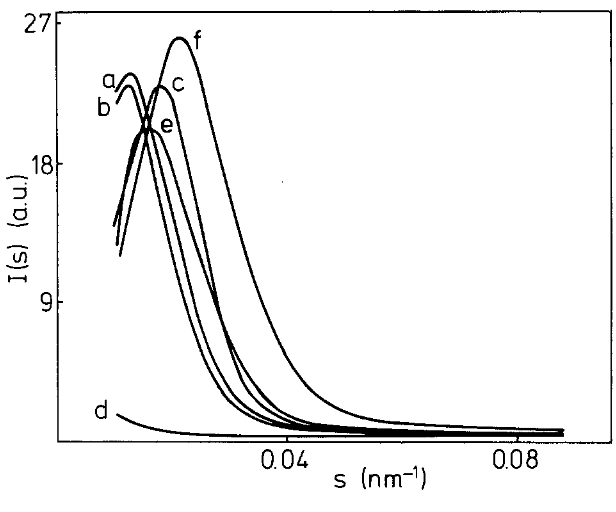


Fig. 9. Meridional SAXS intensity curves of hot-drawn gel-spun polyethylene fibers prepared at different spinning conditions and drawn to different hot-draw ratios $\lambda$. a) $T_{spin}$ = 172 °C, $V_{spin}$ = $V_{wind}$ = 100 m/min, 1.5 wt% HifaxB, $\lambda$ = 4; b) $T_{spin}$ = 180 °C, $V_{spin}$ = 100 m/min, $V_{wind}$ = 500 m/min, 1.5 wt% HifaxB, $\lambda$ = 2; c) $T_{spin}$ = 191 °C, $V_{spin}$ = $V_{wind}$ = 1 m/min, 1.5 wt% HifaxB, $\lambda$ = 5; d) $T_{spin}$ = 172 °C, $V_{spin}$ = $V_{wind}$ = 100 m/min, 1.5 wt% HifaxB, $\lambda$ = 40; e) $T_{spin}$ = 215 °C, $V_{spin}$ = 100 m/min, $V_{wind}$ = 1000 m/min, 5.0 wt% HifaxA, $\lambda$ = 2; f) $T_{spin}$ = 170 °C, $V_{spin}$ = $V_{wind}$ = 1 m/min, 5.0 wt% HifaxA, $\lambda$ = 5.

The same is true for the Porod plots. This is in clear contrast to the results for the extracted fibers considered in section 3.2 (cf. Fig. 4).

Fig. 9 presents meridional intensity curves of fibers prepared at different spinning conditions and drawn to different hot-draw ratios. The relative intensities are again normalized with respect to the sample mass. The meridional intensity curves of fibers originally containing a shish-kebab structure (9b, e) or a lamellar structure (9a, c, f) drawn to low hot-draw ratios contain a clear maximum. This shows that a considerable amount of lamellar material is still present. The amount of backbone material compared to the amount of overgrowth must have been small for the shish-kebab containing fiber. This conclusion is confirmed by the melting experiments on constrained extracted fibers [18]. Drawing to higher draw ratios leads to a reduction of the intensity of the maximum due to a transformation of the lamellar overgrowth into fibrils. The position is hardly affected. These results are in agreement with those obtained by van Hutten et al. [35] except for the fact that in our case no initial increase of the intensity of the maximum as a function of the hot-draw ratio $\lambda$ was observed.

For fibers not stretched in the spinline or stretched in the spinline at relative high spinning temperatures this maximum vanishes completely as shown by curve 9d. This was also checked by using a 40 $\mu$ entrance slit which allows the observation of scattering at still smaller angles. The transformation of lamellar material into fibrils is most probably complete. Conclusions of this kind should always be confirmed by additional means because distortions of the lamellar stackages in the overgrowth by shear may also be responsible. This was found for instance for surface-growth fibers drawn at 90 °C to a very low ratio [33]. In our case, additional evidence was obtained by DSC experiments [17]. However, for hot-drawn fibers originally containing a shish-kebab structure, the maximum does not vanish completely. The transformation of the lamellar structure into fibrils is incomplete and this is particularly true for fibers with very small maximum hot-draw ratios (9b, 9e). This observation confirms the results of melting experiments on these hot-drawn fibers which show a clear low temperature melting peak caused by the melting of lamellae [17].

The position of the meridional maximum is a measure for the period of the stacks of lamellae. It depends on the spinning conditions. The corresponding Bragg values vary from about 48 to 80 nm. The position of the maximum for HifaxB ($\overline{M}_w/\overline{M}_n \approx 3$) is found at smaller angles than for HifaxA ($\overline{M}_w/\overline{M}_n \approx 20$). No significant effect of the polymer concentration could be detected in the concentration range of 1.5–5.0 wt%. Furthermore, there is a tendency for the maximum to shift to smaller angles for a spinning speed of 100 m/min compared to 1 m/min. On the other hand no significant difference between the positions of the maxima for fibers originally containing shish-kebab structure or lamellar structure could be detected. It is well known [41] that polymer systems submitted to various thermal treatments or deformations exhibit memory effects. The time for reaching the equilibrium state in the melt can be several hours. Previous work already showed that the position of the meridional maximum depended on the crystallization temperature, temperature of the melt, cooling rate, and annealing temperature [42]. During the hot-drawing rates process these variables play a role also because, in spite of comparable hot-drawing rates (determined by the wind-off and take-up speed [43]), the deformation, melting and recrystallization inside the hot-draw tube may be different for different fibers. However, the overall process is too complex to give a straight forward explanation of the differences observed. Therefore, meridional SAXS measurements cannot discriminate between fibers drawn to low hot-draw ratios. From this observation we conclude that the presence of small structural differences such as accumulation of entanglements or tight knots [44] and the presence of the molecules in the disordered domains of the backbone fibrils should be responsible for the large differences of the properties found after hot-drawing to the maximum draw ratio.

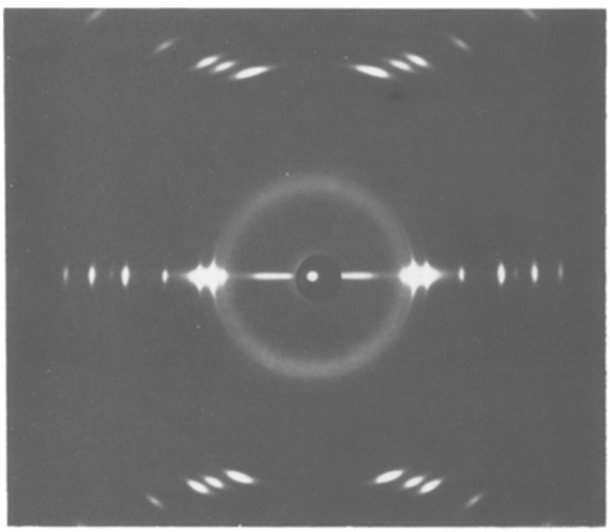

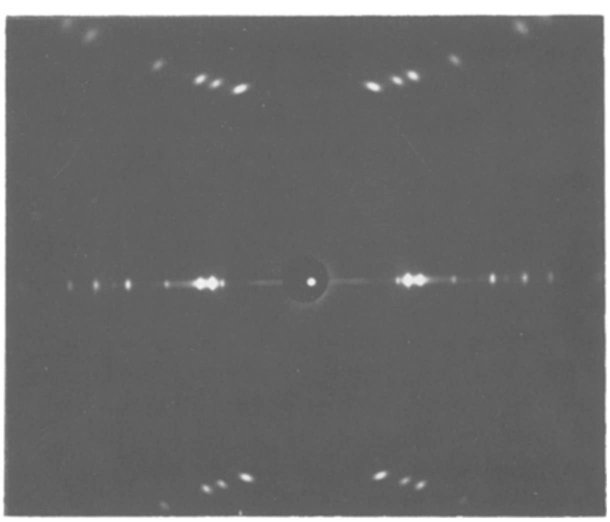

Fig. 10. WAXS diffraction patterns of hot-drawn gel-spun polyethylene fibers prepared at different spinning conditions from a 1.5 wt% HifaxB solution and afterwards drawn to different hot-draw ratios $\lambda$. Fiber axis vertical. a) $T_{spin}$ = 180 °C, $V_{spin}$ = 100 m/min, $V_{wind}$ = 500 m/min, $\lambda$ = 3; b) $T_{spin}$ = 250 °C, $V_{spin}$ = $V_{wind}$ = 1 m/min, $\lambda$ = 40.

In addition to the attempts to distinguish between hot-drawn fibers containing originally shish-kebab or lamellar structure with aid of SAXS, WAXS experiments on hot-drawn fibers were also carried out. Although WAXS turned out to be an excellent technique to distinguish between lamellar and shish-kebab structures in the extracted fibers, this is not longer the case for fibers hot-drawn to the maximum hot-draw ratio. The degree of preferential c-axis orientation parallel to the fiber axis increases with increasing hot-draw ratio in both cases and the intensity of the halo due to the presence of a considerable amount of amorphous material decreases with increasing hot-draw ratio. Only fibers originally containing shish-kebab structures with a very low maximum hot-draw ratio (Fig. 10a) can be distinguished easily from fibers originally containing lamellar structures drawn to high draw ratios (Fig. 10b) due to a less perfect orientation and the presence of a clear halo in the former case.

## Conclusion

We have demonstrated that SAXS is a suitable technique to characterize the morphology of polyethylene fibers during different steps of the gel-spinning process. Different morphologies result from different preparation conditions. Meridional SAXS experiments can distinguish between lamellar and shish-kebab structures in the paraffin oil containing fibers because the intensity curves contain a shoulder for the latter type of structure. After extraction with hexane, void scattering dominates the equatorial and meridional SAXS intensities. Shish-kebab and lamellar structure can only be distinguished by filling the pores with paraffin oil, or by equatorial Porod plots. In the former case, shish-kebab structures show again a meridional shoulder, whereas lamellar structures show an equatorial shoulder/maximum due to tilting of the lamellae during the extraction of the fiber, keeping its length fixed.

After hot-drawing to low hot-draw ratios, fibers containing originally lamellar or shish-kebab structure can no longer be distinguished. Only after hot-drawing to the maximum hot-draw ratio do the meridional scattering curves give some information. Hot-drawing of shish-kebab structures very often lead to low draw ratios and incomplete transformation of the lamellar overgrowth into a fibrillar structure. Relatively weak fibers are obtained. The presence of lamellar overgrowth results in a meridional SAXS maximum shoulder. On the other hand, lamellar structures preferentially oriented with the c-axis perpendicular to the fiber axis can be easily hot-drawn to high draw ratios by chain unfolding. This leads to a nearly complete transformation into fibrils and an meridional SAXS maximum is no longer present. These fibers have excellent properties.

*Acknowledgement*

This study was supported by the Netherlands Foundation of Chemical Research (SON) with financial aid from the Netherlands Organization for the Advancement of Pure Research.

**References**

1. Pennings AJ, Smook J, de Boer J, Gogolewski S, van Hutten PF (1984) in: Seferis JC, Theocaris PS (eds) Interrelations between processing, structures and polymer properties of polymeric materials, Elsevier Science Publishers, Amsterdam, p285
2. Barham PJ, Keller A (1985) J Mater Sci 20:2281
3. Lemstra PJ, Kirschbaum R (1985) Polymer 26:1372
4. Smith P, Lemstra PJ, Kalb B, Pennings AJ (1979) Polym Bull 1:733
5. Kalb B, Pennings AJ (1980) J Mater Sci 15:2584
6. Savitskii AV, Gorshkova IA, Frolova IL, Smikk GN, Loffa IF (1984) Polym Bull 12:195
7. Roukema M, Tillema O, Pennings AJ, to be published
8. Capaccio G, Gibson AG, Ward IM (1979) In: Ciferri A, Ward IM (eds) Ultra high modulus polymers, Applied Science Publishers, London, p1
9. Perkins WG, Capiati NJ, Porter RS (1976) Polym Eng and Sci 16:3
10. Capaccio G, Compton TA, Ward IM (1976) J Polym Sci, Polym Phys Ed 14:1641
11. Zwijnenburg A, Pennings AJ (1976) J Polym Sci (letters) 14:339
12. Smith P, Lemstra PJ (1980) Polymer 21:1341
13. Kanamoto T, Tsuruta A, Tanaka K, Takeda M, Porter RS (1988) Macromolecules 21:470
14. Hoogsteen W, van der Hooft RJ, Postema AR, ten Brinke G, Pennings AJ (1988) J Mater Sci 23:3459
15. Hoogsteen W, Kormelink H, Eshuis G, ten Brinke G, Pennings AJ (1988) J Mater Sci 23:3467
16. Pennings AJ, van der Hooft RJ, Postema AR, Hoogsteen W, ten Brinke G (1986) Polym Bull 16:167
17. Hoogsteen W, ten Brinke G, Pennigs AJ (1988) Coll Polym Sci 266:1003
18. Hoogsteen W, ten Brinke G, Pennings AJ (1987) Polym 28:293
19. Dijkstra DJ, Torfs JC, Pennings AJ Coll Polym Sci, submitted
20. Keller A, O'Conner A (1957) Nature 180:1290
21. Smith P, Lemstra PJ, Pijpers JPL, Kiel AM (1981) Coll Polym Sci 259:1970
22. Matsuo M. Tsuji M, Manley RstJ (1983) Macromolecules 16:1505
23. Matsuo M, Sawatari C, Iida M, Yoneda M (1985) Polymer Journal 17:1197
24. Ciccariello S, Goodisman J, Brumberger H (1988) J Appl Cryst 21:117
25. Porod G (1967) In: Brumberger H, Gordon, Breach (eds) Small angle x-ray scattering, New York, p1
26. Tchoubar D, Mering J (1969) J Appl Cryst 2:128
27. Zwijnenburg A, van Hutten PF, Pennings AJ, Chanzy HD (1978) Coll Polym Sci 256:50
28. Brochard-Wyart F, De Gennes PG (1988) C.R. Acad Sci Paris 306:699
29. Roukema M, Pennings AJ, to be published
30. Van Hutten PF, Koning CE, Pennings AJ (1984) Coll Polym Sci 262:525
31. Van Hutten PF, Koning CE, Pennings AJ (1985) J Mater Sci 20:1556
32. Van Hutten PF, Koning CE, Pennings AJ (1983) Makromol Chem Rapid Commun 4:605
33. Smook J, Torfs JC, van Hutten PF, Pennings AJ (1980) Polym Bull 2:293
34. Van Hutten PF, Pennings AJ (1980) Makrom Chem Rapid Commun 1:477
35. Van Hutten PF, Koning CE, Smook J, Pennings AJ (1983) Polymer 24:237
36. Kambour RP (1973) J Polym Sci, Macromol Rev 7:1
37. Fischer L, Haschberger R, Ziegeldorf A, Ruland W (1982) Coll Polym Sci 260:174
38. Parratt LG (1954) Phys Review 95:359
39. Westbrook PA, Fellers JF, Cakmak M, Lin JS, Hendricks RW (1983) J Polym Sci, Polym Phys Ed 21:1913
40. Hoogsteen W, ten Brinke G, Pennings AJ J Mater Sci, submitted
41. Rault J (1986) CRC Critical Reviews in Solid State and Materials Science 13:57
42. Van Hutten PF, Pennings AJ, Kiel AM (1982) J Mater Sci 17:3525
43. Smook J, Torfs JCM, Pennings AJ (1981) Makromol Chem 182:3351
44. De Gennes PG (1979) In: Scaling concepts in polymer physics, Cornell univ press, ch 6

Received January 16, 1989;
accepted September 9, 1989

Authors' address:

Dr. G. ten Brinke
Dept. of Polymer Chemistry
University of Groningen
Laboratory of Polymer Chemistry
Nijenborgh 16
9747 AG Groningen,
The Netherlands